Available online at www.sciencedirect.com
SCIENCE DIRECT
Tectonophysics 420 (2006) 371–387
TECTONOPHYSICS
www.elsevier.com/locate/tecto

The identification of an active fault by a multidisciplinary study at the archaeological site of Sagalassos (SW Turkey)

Dominique Similox-Tohon [a,1], Manuel Sintubin [a,*], Philippe Muchez [a,1], Griet Verhaert [a,1], Kris Vanneste [b,2], Max Fernandez [c,3], Sara Vandycke [d,4], Hannelore Vanhaverbeke [e,5], Marc Waelkens [e,5]

[a] *Geodynamics and Geofluids Research Group, K.U.Leuven, Celestijnenlaan 200E, 3001 Leuven, Belgium*
[b] *Royal Observatory of Belgium, Ringlaan 3, 1180 Brussel, Belgium*
[c] *Geology Department, Royal Museum for Central Africa, Leuvense steenweg 13, 3080 Tervuren, Belgium*
[d] *Service de Géologie Fondamentale et Appliquée, Faculté Polytechnique de Mons, 9 rue de Houdain, 7000 Mons, Belgium*
[e] *Department of Archaeology, K.U.Leuven, Blijde Inkomststraat 21, 3000 Leuven, Belgium*

Received 22 March 2005; received in revised form 5 February 2006; accepted 18 March 2006
Available online 23 May 2006

Abstract

The archaeological site of Sagalassos (SW Turkey) is located in a region characterized by the absence of any significant recent seismic activity, contrary to adjacent regions. However, the assessment of earthquake-related damage at the site suggests that the earthquakes that have been demonstrated to have struck this Pisidian city in ca. AD 500 and in the middle or second half of the 7th century AD are characterized by an MSK intensity of at least VIII and occurred on a fault very close to the city. Different investigation techniques (archaeoseismology, remote sensing and geomorphology, surface geology and structural data, 2D resistivity imaging and palaeoseismological trenching) have been applied at the archaeological site and its direct surroundings in search for the causative fault of these earthquakes. This multidisciplinary approach shows that each of the different approaches independently provides only partial, non-conclusive information with respect to the fault identification. Integration is imperative to give a conclusive answer in the search for the causative fault. This study has, indeed, revealed the existence of a to date unknown active normal fault system passing underneath ancient Sagalassos, i.e. the Sagalassos fault. A historical coseismic surface rupture event on this fault could be identified. This event possibly corresponds to the devastating Sagalassos earthquakes of ca. AD 500 and the middle or second half of the 7th century AD. Finally, this study demonstrates that in the particular geodynamic setting of

* Corresponding author. Tel.: +32 16 32 64 47; fax: +32 16 32 29 80.
E-mail addresses: dominique.similox-tohon@geo.kuleuven.be (D. Similox-Tohon), manuel.sintubin@geo.kuleuven.be (M. Sintubin), philippe.muchez@geo.kuleuven.be (P. Muchez), griet.verhaert@geo.kuleuven.be (G. Verhaert), kris.vanneste@oma.be (K. Vanneste), max.fernandez@africamusem.be (M. Fernandez), sara.vandycke@fpms.ac.be (S. Vandycke), Hannelore.Vanhaverbeke@arts.kuleuven.be (H. Vanhaverbeke), Marc.Waelkens@arts.kuleuven.be (M. Waelkens).
[1] Fax: +32 16 32 29 80.
[2] Fax: +32 2 373 03 39.
[3] Fax: +32 2 769 54 32.
[4] Fax: +32 65 37 46 10.
[5] Fax: +32 16 32 50 94.

0040-1951/$ - see front matter
doi:10.1016/j.tecto.2006.03.026

SW Turkey archaeological sites with extensive earthquake-related damage form an important tool in any attempt to asses the seismic hazard.

Keywords: Archaeoseismology; Seismotectonics; Active normal faulting; Historical earthquakes; SW Turkey; Fethiye–Burdur fault zone

1. Introduction

Seismic hazard in Turkey (GSHAP, 2004) to a large extent reflects the geodynamics of Turkey (Fig. 1). Both the North- and East Anatolian faults generate first-degree hazard zones. This seismic hazard has indeed in recent history been evidenced by several large earthquakes (e.g. the Izmit and Düzce earthquakes in 1999) (Ambraseys, 2001).

But also SW Turkey figures on this map as a first-degree hazard zone, though not as clearly demarcated as in the case of the North- and East Anatolian faults. We focus on a SW–NE-trending hazard zone extending from Fethiye in the southwest towards the region of the Lakes (i.e. Burdur and Isparta) in the northeast (Fig. 1). The seismicity — and thus the seismic hazard — is considered to be related to a particular tectonic feature, the so-called Fethiye–Burdur fault zone (Barka et al., 1995; Bozkurt, 2001) (Fig. 1). Although the Fethiye–Burdur fault zone is identified as a region with high seismic hazard, it is associated with weak to moderate earthquakes. In the last century, no large events ($M > 6.0$) have been registered along the entire middle section of the fault zone. Only at the northeastern extremity

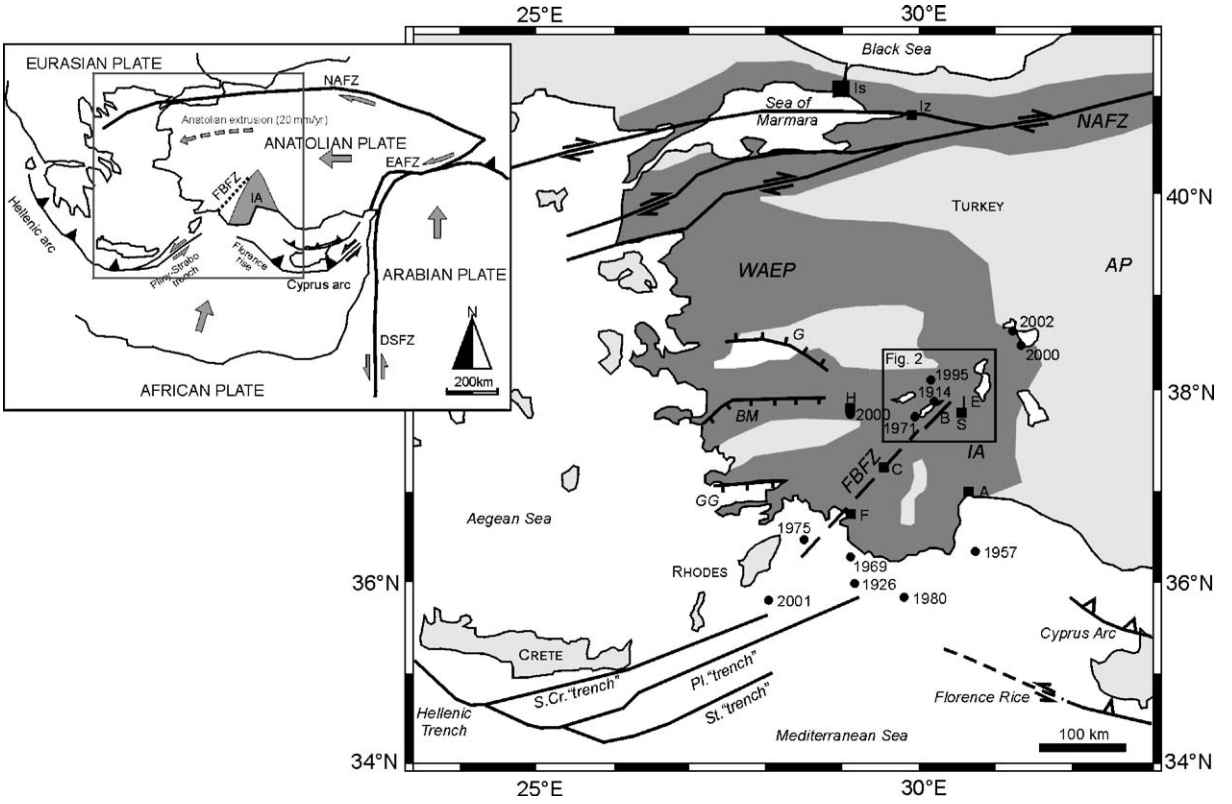

Fig. 1. Tectonic setting of the Fethiye–Burdur fault zone (FBFZ) in SW Turkey. Major tectonic structures are indicated (after ten Veen, 2004). The FBFZ is located in the first-degree hazard zone, marked in dark grey (10% probability of exceeding in 50 years peak ground accelerations of 4.0 m/s^2) (GSHAP, 2004). Large ($Ms \geq 6.0$) earthquakes since 1900 nearby the FBFZ are indicated (Ambraseys, 2001; KOERI, 2002; Emre et al., 2003). NAFZ: North Anatolian fault zone; WAEP: Western Anatolian extensional province; AP: Anatolian Plateau; IA: Isparta Angle; G: Gediz graben; BM: Büyük Menderes graben; GG: Gokova Graben; Is: Istanbul; Iz: Izmit; H: Hierapolis; B: Burdur; I: Isparta; E: Egridir; S: Sagalassos; C: Cibyra; F: Fethiye; A: Antalya. Inset: geodynamic model of the Eastern Mediterranean tectonics. NAFZ: North Anatolian fault zone; EAFZ: East Anatolian fault zone; DSFZ: Dead Sea fault zone; FBFZ: Fethiye–Burdur fault zone; IA: Isparta Angle.

(Burdur 1914 and 1971, Dinar 1995, Afyon 2000 and 2002, Dinizli 2000) and at the — off-shore — southwestern extremity (Rhodes 1957, off-shore Turkey 1926, 1969, 1975, 1980 and 2001) large earthquakes occurred. The entire central segment of the Fethiye–Burdur fault zone is seismically quiescent, suggesting the presence of a seismic gap in this central segment (Fig. 1).

Southwest Turkey is densely covered by Hellenistic, Roman, Byzantine, Selcuk and Ottoman archaeological sites. Evidences of earthquake-related damage in these archaeological sites (e.g. Hancock and Altunel, 1997; Altunel, 1998; Waelkens et al., 2000; Akyüz and Altunel, 2001; Altunel et al., 2003) offer the unique opportunity to trace back in historical times the seismic activity. Archaeoseismological evidence subsequently allows to extend our knowledge on the seismic history. Archaeological sites in the Fethiye–Burdur fault zone, such as Cibyra (Akyüz and Altunel, 2001) and Sagalassos (Waelkens et al., 2000), indeed show that large earthquakes did occur historically on the central seemingly seismically quiescent segment of the fault zone (Fig. 1), thus documenting the occurrence of potentially hazardous faults capable to generate large earthquakes.

A major limitation of potentially archaeoseismological evidence is that it does not allow the identification of the causative, thus hazardous, fault. Often only assumptions are made with respect to the fault on which the devastating earthquake occurred (e.g. Hancock and Altunel, 1997; Altunel, 1998; Waelkens et al., 2000; Akyüz and Altunel, 2001; Altunel et al., 2003).

A multidisciplinary approach is imperative to identify active faults (e.g. Caputo, 1996; Collettini et al., 2003), in which archaeoseismology can possibly play a significant role to the extent that archaeoseismological evidence even becomes a proxy for active faults.

In this paper we want to present the results of such an integrated approach on the ancient city of Sagalassos, located some 10 km south–southwest of Isparta (Fig. 1). At ancient Sagalassos, archaeoseismological evidence suggests the occurrence of two historical earthquakes (Waelkens et al., 2000; Sintubin et al., 2003). It is believed that Sagalassos was located within the epicentre of the two earthquakes, causing major and widespread damage. We document that each of the different approaches independently does not give a conclusive answer and that only their integration allows the identification of the active fault. In the case of Sagalassos it is also documented that the integration of results from archaeoseismology, remote sensing and geomorphology, surface geology and structural data, geophysics and palaeoseismological trenching revealed that the Sagalassos site stands on an active normal fault system, i.e. the Sagalassos fault. Eventually, this integrated approach evidences that in the particular geodynamic setting of SW Turkey archaeoseismological data can indeed be used as a supplementary tool in a seismic hazard assessment of the region.

2. Geodynamic and seismotectonic setting

The ancient city of Sagalassos is located in the northeastern sector of the Fethiye–Burdur fault zone. The left-lateral transtensional Fethiye–Burdur fault zone is considered the northeastern continuation of the offshore Pliny–Strabo trench (e.g. Barka et al., 1995; Bozkurt, 2001), therefore representing the plate boundary between the subducting African plate and the Aegean–Anatolian/Eurasian plate (Fig. 1). In this geodynamic model, the Fethiye–Burdur fault zone is interpreted as the crustal expression of a lithospheric lateral tear fault, caused by the detachment of the subducting plate underneath the eastern Taurus (Barka et al., 1995). Although suggested by GPS measurements, the left-lateral kinematics of the Fethiye–Burdur fault zone remains controversial (Barka et al., 1995; Barka and Reilinger, 1997; Kahle et al., 1999; Bozkurt, 2001). To the west, the Fethiye–Burdur fault zone delimits the Aegean–West Anatolian extensional province, where the geodynamics — and thus the seismicity — is dominated by major, predominantly EW-trending normal fault systems (e.g. Menderes, Gokova, …) (Fig. 1).

On the other hand, the Fethiye–Burdur fault zone forms the western boundary of the so-called Isparta angle (Blumenthal, 1963), a complex triangular-shaped tectonic domain that resulted from Cretaceous to Late Miocene accretion tectonics (Robertson, 1993; Collins and Robertson, 1997) (Fig. 1). The junction between both the Hellenic and Cyprus arcs and its geodynamic implications with respect to the tectonics of the Isparta angle is still a matter of debate (Barka et al., 1995; Glover and Robertson, 1998). Recent research on Crete (ten Veen and Kleinspehn, 2003) and Rhodes (Greece) (ten Veen and Kleinspehn, 2002) and in the Fethiye area on mainland Turkey (ten Veen, 2004) sheds new insights on the complex geodynamics of the Pliny–Strabo trench and its possible northeastern link with the Fethiye–Burdur fault zone. In this new geodynamic model, the dominant features are rhomb-shaped basins in an overstepping geometry, bounded by N70- and N20-trending faults. These basins formed in an overall left-lateral transtensional setting related to the increasing

plate-boundary curvature leading to an increasing obliquity of convergence and to the incipient continental collision of an African continental promontory south of Crete. This collision gives rise to a northeastward propagating transcurrent motion of forearc slivers sheared off along the eastern side of the expanding forearc (Fig. 1). A main question to be resolved is whether or not this geodynamic model can be extended to the northeast, possibly explaining the geodynamics of the entire Fethiye–Burdur fault zone. Recent work (Sintubin et al., 2003) suggests the presence of both orientations of basin-bounding faults in the northeastern extremity of the Fethiye–Burdur fault zone in the Burdur–Isparta area.

The current extensional regime started in Late Miocene–Early Pliocene time (Bozkurt, 2001) and is classically related to the westward motion of the Anatolian plate towards the Aegean region, which is caused by the northward impingement of the Arabian plate into the Eurasian plate (Fig. 1). However, classic plate tectonic models of the Aegean region, with purely horizontal movement, should be considered carefully (Pavlides and Caputo, 1994). A mechanical paradox emerges by the occurrence of extension where compression should regionally, or at least locally, predominate due to the westward convergence of Anatolia and the subduction along the Hellenic arc (Pavlides and Caputo, 1994). At the northeastern extremity of the Fethiye–Burdur fault zone this extensional regime is expressed by three NE–SW trending half grabens, bounded by major NW-dipping normal faults, the Burdur, Acıgöl and Baklan faults (Price and Scott,

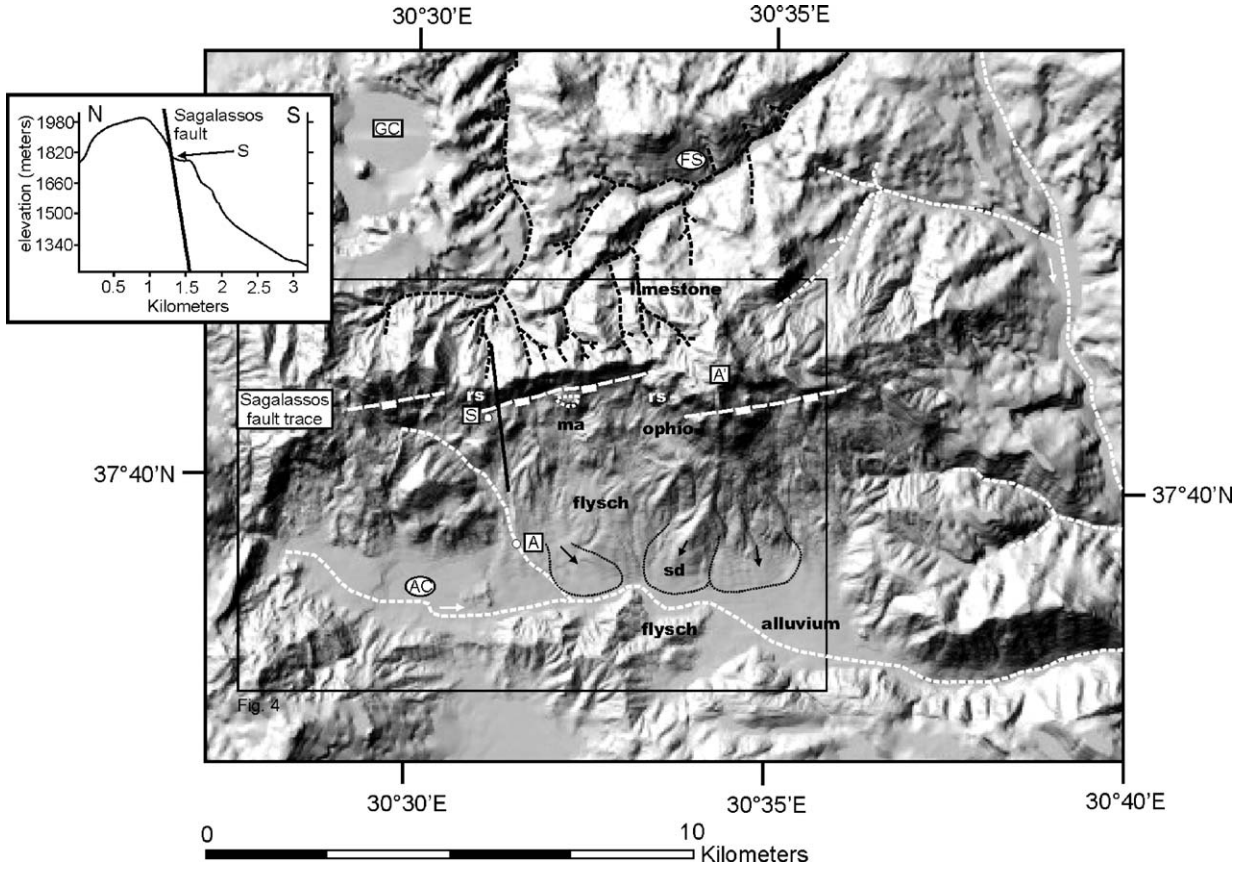

Fig. 2. Geodynamic setting of the Sagalassos fault (SF) as fault linkage between the northeastern Fethiye–Burdur fault zone (FBFZ) and the Isparta–Eğridir fault zone (IEFZ) showing major structural elements, epicentres of recent major earthquakes with known causative fault (stars), epicentres of recent major earthquakes with unknown causative fault (triangle), location of historical seismic activity (squares), available focal mechanisms, isoseismal contours with the intensity VIII (after Taymaz and Price, 1992; Eyidoğan and Barka, 1996) and NE–SW-elongated cluster of recent (1900–2000) micro-seismic activity (white circles are Md 3.0–3.9 events and grey circles represent Md 4.0–4.9 events after KOERI, 2002) along the IEFZ. Open arrows indicate the overall NW–SE-trending extensional deformation in the Burdur–Isparta area, black arrows show the deformation regime for the Sagalassos fault, FBFZ and IEFZ. Left-lateral movement on the Sagalassos fault is indicated by the en-échelon arrangement of the Sagalassos fault segments.

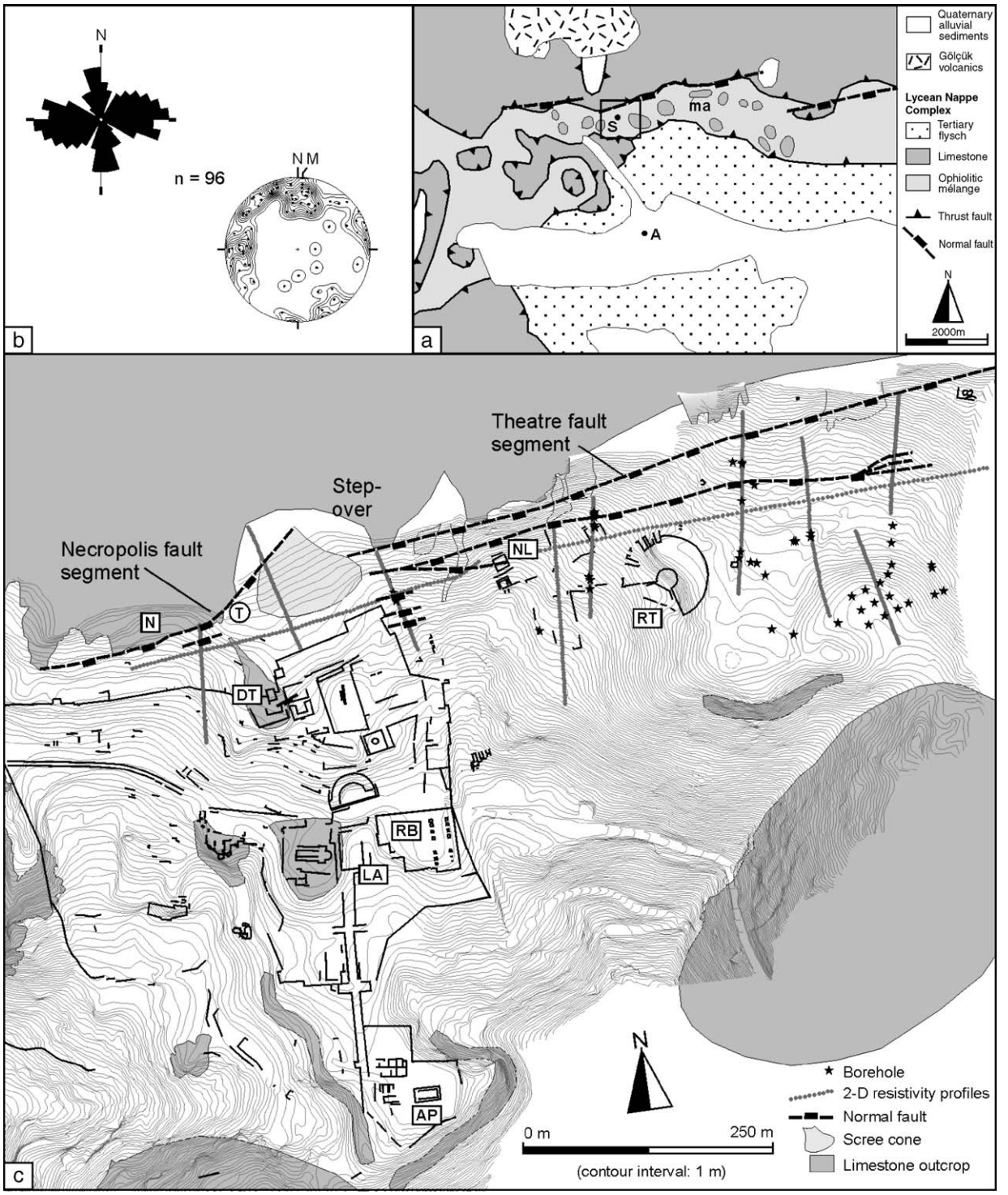

Fig. 3. Digital elevation model of the region around ancient Sagalassos (illuminated from the NW), showing the location of the three Sagalassos fault segments and their right-lateral step overs (rs), the footwall streams (FS), the Ağlasun Çayı river (AC) the Gölcük Crater (GC), the slumped massif of the aqueducts (ma), the large slope deposits (sd), the major geological units (limestone, ophiolite, flysch and alluvium), the Akdağ mountain at 2271 m a.s.l. (A′), the village of Ağlasun at 1150 m a.s.l. (A), the ancient city of Sagalassos (S) and outline of Fig. 4a. Black line indicates location of topographic profile. Inset: digital topographic profile across the Sagalassos fault (vertical exaggeration 1:2.5).


a

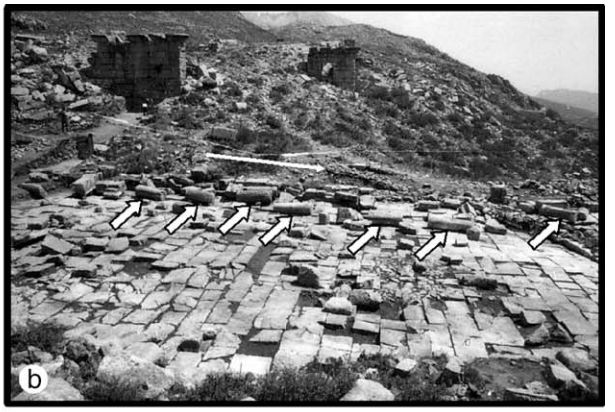
b


15°
c


d


15°
e

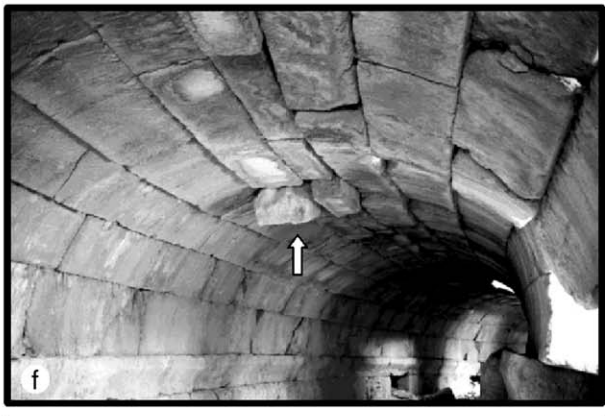
f


g

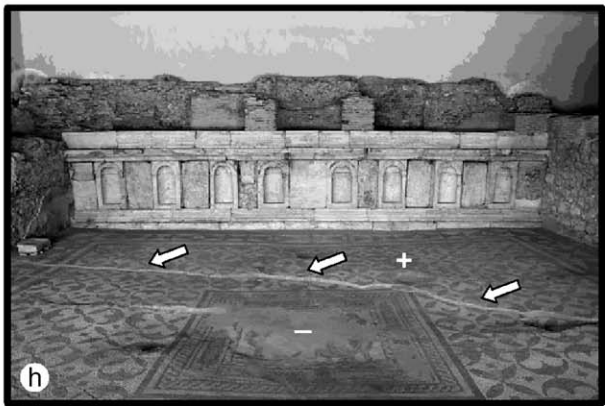
+
−
h

1994) (Figs. 1 and 2). Quaternary basins developed within these grabens. These basins occupy the central part of wider, fault-bounded Pliocene basins (Price and Scott, 1991). To the northeast, the graben system terminates against the NW–SE trending Dinar fault, considered as a break-away fault within this system (Figs. 1 and 2). Large earthquakes occurred in 1500 BC, 80 BC and 1995 on the Dinar fault, in 1875, 1925 and 1933 on the Baklan fault and in 1914 and 1971 on the Burdur fault (Altunel et al., 1999; Koral, 2000; Ambraseys, 2001). The seismogenic fault(s) responsible for several other earthquakes have not been identified yet (Fig. 2; Similox-Tohon et al., 2005).

3. Remote sensing and geomorphology

The Ağlasun Dağları mountain range-front, north of the Ağlasun valley, can clearly be recognized on the LANDSAT and ASTER satellite images, aerial photographs (1:40,000-scale) and DEM (obtained by manually digitizing 1:25,000-scale topographic maps, resulting in an accuracy of 10 m) as a ca. 10 km-long, ENE–WSW–trending lineament consisting of three right-stepping en-échelon segments (Fig. 3). The top of this mountain range forms a nearly flat plateaux at a mean altitude of 2000 m a.s.l. where the highest summit is the Akdağ (2271 m), whereas the Ağlasun valley floor lies at about 1150 m a.s.l. The valley is dominated by the south-facing continuous and nearly undissected cliffs of white limestone, which surmount gentler footslopes in ophiolitic material and flysch deposits. The steep limestone front is about 250 m high at the northern limit of Sagalassos. In sharp contrast with the undissected and continuous southern slopes, the limestone mountains are heavily dissected by important valley systems directed northward (Fig. 3). Paulissen et al. (1993) explained this asymmetric section as a result of the gently dipping limestone sheet towards the north between Sagalassos and Isparta and hence considered the south-facing limestone front as a cuesta front. However, it could equally represent a south-dipping active normal fault, characterized by a footwall stream pattern due to back-tilting of the footwall (cf. Goldsworthy and Jackson, 2000). A strong geomorphological resemblance exists between the Ağlasun Dağları mountain range-front and active normal faults in the Aegean region where footwalls are hard and resistant (e.g. limestone) (Goldsworthy and Jackson, 2000). Moreover, the morphology of the Ağlasun Dağları mountain range-front, as recognized on satellite images and DEM, is very similar to known nearby active normal faults in limestone, such as the Acıgöl or the Eğridir faults (Fig. 2). Therefore it is likely that the Ağlasun Dağları mountain range-front represents the geomorphological expression of the Sagalassos fault.

Various present-day geomorphological processes are active on the south-facing mountain slopes (Paulissen et al., 1993). Evidence of extensive mass movement processes (e.g. soil creep, rockfalls and rock slides, debris flows and/or avalanches, mudflow) are described by Librecht et al. (2000) and Paulissen et al. (1993). Several processes were already active in historical and pre-historical times (e.g. slumped limestone massifs, cemented fossil rockfall talus; Librecht et al., 2000; Verstraeten et al., 2000). The most spectacular historical event is a slumped limestone massif east of Sagalassos (Figs. 3 and 4), where parallel aqueducts, ca. 7 m apart, can be observed (Steegen et al., 2000). The upper aqueduct is still in line with the rest of the eastern aqueduct and is less weathered than the lower aqueduct, thus suggesting a younger age. To date, the original construction of only one entire aqueduct east of the city is known. Accordingly, the presence of two aqueduct segments is interpreted as an evidence of a slumping event that occurred during historic times. The fact that street levels were raised and an effort was made to provide the city with new water-supply systems after ca. AD 500 shows that the large earthquake in ca. AD 500 caused a water shortage in the city (Waelkens et al., 2000). This earthquake could have possibly triggered the landslide that interrupted the eastern aqueduct (Sintubin et al., 2003).

In front of the central and eastern segment of the Sagalassos fault, more or less cone-shaped large debris slopes reached the Ağlasun valley bottom and made the Ağlasun Çayı river shift towards the southern flysch hills (Fig. 3; Six, 2004). The Ağlasun Dağları mountain range-front can be interpreted as a “seismic landscape” (defined as the cumulative geomorphological and stratigraphical effect of signs left on the environment

Fig. 4. Structural analysis. (a) Simplified geological map (after Degryse et al., in press) of the region around ancient Sagalassos (see Fig. 3 for location), showing the location of the three Sagalassos fault segments, the slumped massif of the aqueducts (ma), the village of Ağlasun (A) and the ancient city of Sagalassos (S). The Sagalassos fault affects the frontal parts of the Lycian nappe complex. (b) Rose diagram and equal-area, lower hemisphere projection with contours of the poles of the fractures affecting the footwall block of the Sagalassos fault. (c) Map of the archaeological site of Sagalassos showing the location of the identified fault segments, the resistivity profiles, the trench (T), the drillings, the limestone outcrops, the scree cones, the necropolis (N), the Doric Temple (DT), the Neon library (NL), the Roman Theatre (RT), the Roman Baths (RB), the Lower Agora (LA) and the temple for Antoninus Pius (AP). See (a) for location.

of an area by its past earthquakes over a geologically recent time interval; Michetti and Hancock, 1997; Michetti et al., 2005), in which periods of instability occurred in pre-historical, historical up to recent times. Some of the mass movements along the Ağlasun Dağları mountain range-front could be earthquake-induced and related to activity on the Sagalassos fault, while others represent degradation of the fault face (Sintubin et al., 2003).

In conclusion, the geomorphological analysis suggests the existence of a SSE-dipping active major normal fault bounding the northern margin of the gentler footslopes north of the Ağlasun valley: the Sagalassos fault. Extensive mass movements obscure, however, possible fault scarps that could have documented recent surface-rupturing events on the Sagalassos fault.

4. Surface geology and structural data

The ENE–WSW-trending Sagalassos fault is cross-cutting the frontal parts of the pre-existing Lycian nappe complex, which was emplaced during late Miocene times from the northwest to the southeast (Collins and Robertson, 1997) (Fig. 4). This stack of thrust sheets consists of limestone nappes, which were thrust on top of ophiolitic material, the last thrust on flysch deposits that developed in the foreland basin in front of the prograding Lycian nappes (aenel, 1997). In the north, the thrusts hanging-wall is predominantly made of limestone. Directly to the south, the thrusts footwall is predominantly made of ophiolitic material, while the gentler slopes further south are made of flysch. Quaternary alluvial deposits fill the Ağlasun valley to the south. In the thrusts footwall several limestone platforms occur (Fig. 4). Some represent tectonic lenses (i.e. in situ isolated parts of the limestone nappe on top of the ophiolitic material) and others are the result of macro-slumps. The latter implies slumping of limestone blocks from the limestone front with the sliding surface in the ophiolitic material or on the clayey horizons in the flysch deposits (Paulissen et al., 1993; Verstraeten et al., 2000).

Structural analysis along the Sagalassos fault shows that deformation is characterized by conjugate systems of vertical to sub-vertical fractures, trending normal and parallel to the Sagalassos fault (Fig. 4b). These fractures represent the near-surface shatter zone, which formed during the initial blind faulting at depth, typical of neotectonic normal fault zones cutting bedrock carbonates within the Aegean region (Stewart and Hancock, 1990).

No clear continuous fault plane can be observed along the whole fault length at the surface. However, a number of other observations provide evidence for characterizing the Sagalassos fault. Secondary fault segments are separated by right-lateral stepovers (e.g. Necropolis fault segment and Theatre fault segment; Fig. 4). At places, the limestone scarp may be interpreted as a strongly degraded fault plane. Meso-scale normal faults are ubiquitous along the Sagalassos fault (Fig. 7c). They are commonly steeply dipping but with variable strike. Dip–slip movements prevail although oblique movements are observed. Multiple slip planes are present, indicating several fault reactivations. The mesoscale faults are characterized by a narrow (mm), striated cemented fault breccia and display cm-scale corrugations. Occasionally, comb fractures occur on the slip planes. Underneath the slip plane, a cataclastic zone is present. This brecciation and fracturing along slip planes is characteristic for neotectonic normal fault zones in the Aegean region (Stewart and Hancock, 1990). In the hanging-wall of the Sagalassos fault, fractured and faulted cemented rockfall talus has been observed as evidence for neotectonic activity (Sintubin et al., 2003).

The highly degraded aspect of the Sagalassos fault and the absence of a clear free face might indicate a low slip rate. The lack of a continuous degradational profile across the limestone face, which is expected and observed in several examples of active normal faults in limestone (e.g. Stewart, 1996), is evidence that the fault has not been active in recent times. However, we may assume that mass movements and rapid weathering (3.2–27.8 mm in the steps of the Roman Theatre (2nd century AD), Van de Velde, 1998) with respect to fault activity may have obscured any evidence of recent fault activity.

A palaeostress analysis reveals the occurrence of a transient stress field since late Miocene time in the Burdur–Isparta area (Verhaert et al., 2004). Striated fault planes were measured in 24 structural stations, distributed within the Burdur–Isparta area. The Sagalassos fault represents one of these stations. A semiautomatic procedure has been used for analyzing and separating seven stress tensors from heterogeneous fault-slip data ($n=116$). Although the inversion method is automatic, the separation of the seven stress tensors and therefore homogeneous fault data needed to be carried out manually, so that it can be considered as a semiautomatic procedure, for separating stress tensors. The direct inversion method of Angelier (1984) was used to search for the best tensor to fit for the seven conjugate or quasi-conjugate Andersonian fault systems. The mesoscale structures measured along the Sagalassos fault ($n=81$) mostly belong to the same fault population and are

compatible with a NW–SE trending extension that also represents the present-day stress field of the Burdur–Isparta area (Figs. 2 and 4; cf. Temiz et al., 2001). This is confirmed by the fault plane solutions of the 1971 Burdur and 1995 Dinar earthquakes indicating pure normal dip–slip faulting in a biaxial extensional regime (Fig. 2; Taymaz and Price, 1992; Eyidoğan and Barka, 1996). In such an extensional regime the WSW–ENE-trending Sagalassos fault should be activated with oblique (dip–slip and sinistral) kinematics. The geometry of the three major fault segments and of the secondary stepovers also suggests such sinistral component of movement.

5. Damage in Sagalassos-archaeoseismology

The ancient city of Sagalassos is located at an altitude of 1490–1600 m a.s.l., overlooking the valley of Ağlasun to the south (Fig. 3). The city has been built on ophiolitic material covered by large carbonate klippe and macro-slumps (Paulissen et al., 1993; Verstraeten et al., 2000). The topography of the city is characterized by several large platforms, which are related to these limestone blocks (Fig. 4).

Destruction layers exhibiting extensive damage to major structures are often attributed by archaeologists to large earthquakes. However, structural damage is often less unequivocal than generally assumed. It is essential in the description of ancient damage and in the consideration of its origin, to maintain a proper balance between, geological, geomorphological and geotechnical factors on one hand, and historic, anthropogenic and archaeological factors on the other hand (Karcz and Kafri, 1978; Rapp, 1986). Therefore a thorough archaeoseismological investigation has been conducted at Sagalassos. Although many buildings date from the Hellenistic period, prior to a 1st century AD collapse of buildings, all these buildings were systematically repaired (e.g. Waelkens et al., 2000), so that it is fair to assume that most of the observed earthquake-related damage can be attributed to the seismic catastrophes in ca. AD 500 and in the middle or second half of the 7th century AD. The age of these earthquakes is based on coins and pottery overlain by the collapsed monuments (Waelkens et al., 2000). The damaged buildings consist mostly of very well built structures made of large limestone blocks and therefore only some damage results from inaccurate craftsmanship as e.g. in the ground level of the Roman Baths (Ignoul and Van Gemert, 1999).

Several types of earthquake-related damage have been observed (e.g. Sintubin et al., 2003). First, the buildings are affected by widespread fracturing. Several examples of fractures passing through two or more adjacent blocks are present (cf. Korjenkov and Mazor, 1999a,b) (Fig. 5a). Such throughgoing joints are attributed by Korjenkov and Mazor (1999a,b) to earthquakes with a minimum local intensity of I=VIII (MSK-64 scale). Monolithic columns typically show fracturing caused by axial loading (cf. Stiros, 1996). Second, the columns on the Lower Agora collapsed all in a ~NS direction (Fig. 5b). Third, walls are usually tilted (up to 20°) (Fig. 5c) or even collapsed directionally, leaving in some cases a typical U-shaped gap associated with a symmetrically shaped collapse cone and drag at the remaining wall corners (e.g. Roman Theatre) (Fig. 5d). Exceptionally, a domino-style collapsed wall is present at the Upper Agora. An overall preferential collapse towards the southeast occurred during the youngest event. Fourth, at places, single blocks or parts of the main outside walls are rotated along vertical axes with angles ranging from 5° to 20° (Fig. 5e). Fifth, nearly all the arches and vaults were affected (cf. Stiros, 1996). Keystones have subsided and the voussoirs were displaced relative to each other (Fig. 5f). Exceptionally arches are intact, possibly reflecting a preferential orientation of ground motion. Sixth, some stairways (e.g. Bouleuterion, Domestic area, Lower Agora, Roman Theatre) completely collapsed or were distorted. Finally, holes of missing stones are present in the Roman Theatre and the Doric Temple (Fig. 5g). Korjenkov and Mazor (1999a,b) use such holes as indication of "shooting" or "bursting" resulting from localized stress release during large earthquakes with intensity of at least I=VIII.

Detailed assessment of the damage has revealed that nearly all archaeological relics show different degrees of earthquake-related damage. The archaeological relics affected are spread over an area of 2.5 by 1.2 km. This area is far too large to be affected by e.g. a single event of slope failure. Moreover, the geomorphological setting of several damaged buildings (e.g. Neon Library, Upper Agora and Theatre) is such that no slope process could have had any influence on the constructions (e.g. Waelkens et al., 2000). Moreover, the damaged relics built on both limestone and ophiolitic substrate, show that damage seems to be independent of the nature of the bedrock on which the buildings were constructed.

Ancient buildings usually have only one or two floors. Hence, they are short-period structures that are sensitive to shaking by short-period seismic waves, whose effect is strongly attenuated with distance. Therefore, archaeoseismological data generally record local earthquakes, whose epicentre is up to a few tens of

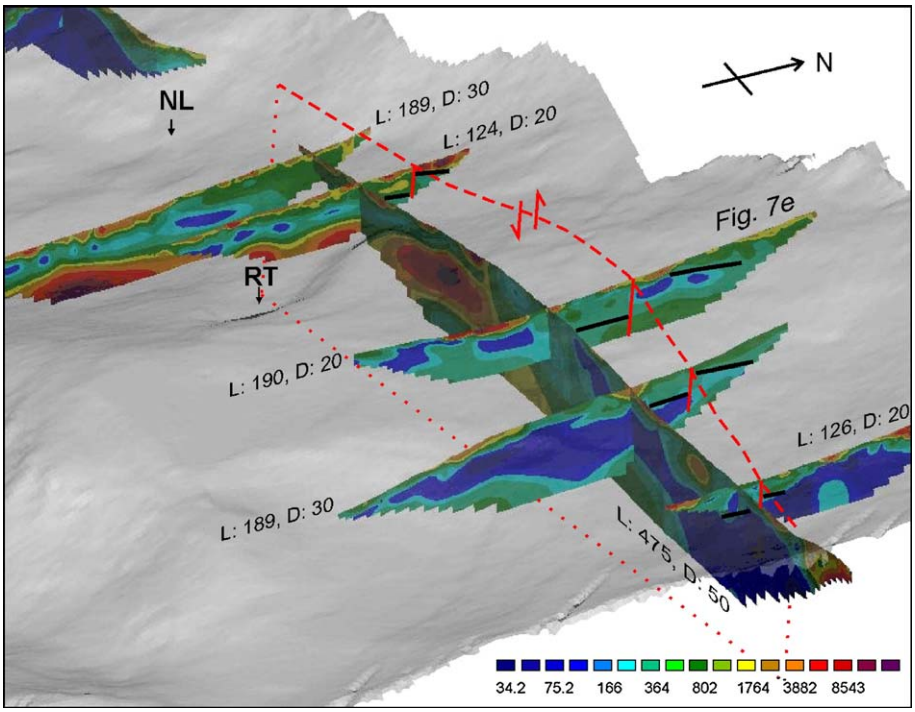

Fig. 5. Examples of earthquake-related damage at ancient Sagalassos. (a) Fractures crossing several adjacent blocks in a doorpost in the Roman Baths (2nd century AD). Such throughgoing joints are attributed by Korjenkov and Mazor (1999a,b) to earthquakes with a minimum intensity of I=VIII. (b) Columns (arrows) on the Lower Agora collapsed all in an ~NS direction (small arrow). (c) Tilted wall (15°) in the Roman Theatre (1st century AD). (d) Directionally collapsed wall in the Roman Theatre (1st century AD), leaving a typical U-shaped gap associated with a symmetrically shaped debris cone and drag effect at the remaining wall corners. (e) Rotation (15°) around a vertical axis of a block in the outer wall of the temple for Antoninus Pius (2nd century AD). (f) Subsided keystones (arrow) in the Vomitorium of the Roman Theatre (1st century AD). (g) Hole of missing stone (arrow) in the western outer wall of the Doric Temple (1st century BC). Korjenkov and Mazor (1999a,b) attribute such holes to earthquakes with intensity of at least I=VIII. (h) Fracture pattern (post-363 AD) in the mosaic floor and walls of the Neon Library. Plus (+) indicates uplifted part and minus (−) indicates subsided part of the floor. See Fig. 4 for location.

kilometers away from the site (Stiros, 1996). In the region, the isoseismal contours with intensity VIII for both the Ms 6.2 1971 Burdur and Ms 6.1 1995 Dinar earthquake are moreover rather localized, while the Ms 7.0 1914 Burdur earthquake affected a larger area (Eyidoğan and Barka, 1996) (Fig. 2). Consequently, the characteristics and distribution of the damage at Sagalassos strongly suggest that they could be related to a seismic event characterized by local intensity I=VIII and macroseismic epicentre close to the site (<20 km).

In the Neon Library, both the mosaic floor and the walls show evidence of normal faulting (Fig. 5h). The fault trace runs approximately E–W (N87°) and throws the southern part of the floor a few centimeters downward. However, one should be very cautious using faulted relics to confirm the existence of an active fault without palaeoseismological or specific geophysical analyses (cf. Hancock and Altunel, 1997; Galli and Galadini, 2001).

6. 2D resistivity imaging

2D resistivity imaging has been used to document the subsurface occurrence and geometry of the fault affecting the Neon Library. This method yields a vertical section of the subsurface resistivity distribution. For the aim of this study, i.e. the detection of steeply dipping normal faults, two different electrode layouts were considered: the Wenner–Schlumberger (WSC) layout and the dipole–dipole (DDP) layout. Both layouts were tested with otherwise identical parameters. The DDP data appeared to be so noisy that they could not be inverted into a reliable model. The WSC layout proved to be the best for the particular conditions at the site of Sagalassos. The electrode spacing along the survey line (i.e. the minimum interelectrode spacing) was chosen to ensure the required resolution and penetration depth, in function of the position of the suspected fault along the profile and the space available. The first profile was laid out with a relatively large

electrode spacing (3 m), which confirmed that the bedrock depth did not exceed 10 m. From this profile, we concluded that a target depth of 20 m was sufficient, and subsequent profiles were carried out with an electrode spacing of 2 m.

Eleven profiles were acquired (Fig. 4). Nine profiles were carried out perpendicular to the suspected fault trace plus two longitudinal profiles connecting the transversal sections. The longitudinal profiles were carried out with a larger electrode spacing (4 and 5 m), in order to overcome the large distances between the transversal sections. The profiles are situated in an area where many archaeological structures and coarse debris, shed from the limestone cliff, are present at the surface and characterized by slopes between 11° and 23°. This hampered an optimal cover of the area.

For each data point, the resistivity meter performs a stack of a minimum of two and a maximum of four measurements. The standard deviation for each stack generally below 2.5% indicates a relatively good quality of the data, considering the difficult conditions. Before proceeding with the inversion, the data set was reduced: all negative resistivity values were rejected, as well as all data points with a standard deviation above a certain threshold. The filtered data were subsequently reevaluated visually, and any remaining isolated extreme value was removed.

The measured resistivity values do not represent the true subsurface resistivity, but an 'apparent' resistivity. Pseudosections plotting the apparent resistivity as a point do not give an accurate picture of the true subsurface resistivity, because these plots do not take into account that the signal of each value measured in fact originates from a volume of the subsurface that depends on the type of array used. Determining the true subsurface resistivity is an inverse problem. All inversions were carried out taking into account the topography along the profile. The large differences in length, elevation and depth of the profiles required a 3D visualization of the data set (Fig. 6). A detailed description of the data acquisition and processing of the 2D resistivity profiles is treated in Similox-Tohon et al. (2004).

The obtained resistivity profiles allow to distinguish five electrical resistivity units (from bottom to top): (a) the bedrock consisting of either limestone or ophiolitic material, (b) the weathered top of this bedrock, (c) old colluvial material, (d) recent colluvial material that covers archaeological structures and (e) recent scree deposits (Figs. 6 and 7e). The proposed stratigraphy is based on the absolute and relative resistivity values of the different resistivity layers and their correlation with borehole data (up to 6 m deep).

Some features that occur systematically on most transversal profiles are indicative of the presence of active normal faults (Figs. 6 and 7e). The clear vertical displacements, up to 10 m, of the bedrock (resistivity unit a) are considered evidence for south-dipping normal faults. The overlying wedge-shaped old colluvial layer (resistivity unit c) displays a sharp termination at the fault contact and also shows a clear vertical displacement. This is indicative of the presence of a fault scarp and thus of surface rupture events that occurred in pre-occupation times. The recent colluvial layer (resistivity unit d) and the recent scree deposits (resistivity unit e) do not seem to be affected by the faults. The faults observed in each profile could be laterally correlated (Figs. 4 and 6) and mapped showing a N80°E trend, nearly parallel to the major limestone scarp and the faults affecting the mosaic floor of the Neon Library. The resistivity profiles provide evidence of several south-dipping synthetic active normal fault strands in a 150-m wide fault zone. Moreover, these faults could have been reactivated during historical times as the normal faults affect both the mosaic floor and the walls of the Neon Library. The faulting of the Neon Library postdates AD 363 and is thought to be the result of the middle or second half of the 7th century AD earthquake (Waelkens et al., 2000). However, no surface evidence is present for the faults identified in the 2D resistivity profiles. The lack of any evidence of fault scarps at the surface may be due to burial by recent colluvium and building material. Most of the present-day topographic scarps correspond to anthropogenic terrace walls. Even though gravitational movements are active around the archaeological site, it is unlikely that the faults in the 2D resistivity profiles represent the sliding surface of rotational slumps. The faults detected on the resistivity profiles represent rather linear fault traces over a distance of at least 550 m. In the case of a slump we would expect a more curved (concave downwards) surface. Moreover, no clear geomorphological expression of such a large-scale rotational slumping is related to these faults (Fig. 4).

The detected displacements in the resistivity profiles are interpreted as minor synthetic faults formed in the hanging-wall block of the major normal Sagalassos fault, therefore representing the common basin-ward migration of fault splays at the surface (e.g. Stewart and Hancock, 1988). However, the large displacement on some faults cannot be the result of one single seismic event. It is more likely that the old colluvial layer (resistivity unit c) consists of several smaller colluvial wedges corresponding to a number of morphogenic earthquakes (Caputo, 1993), though the resolution of

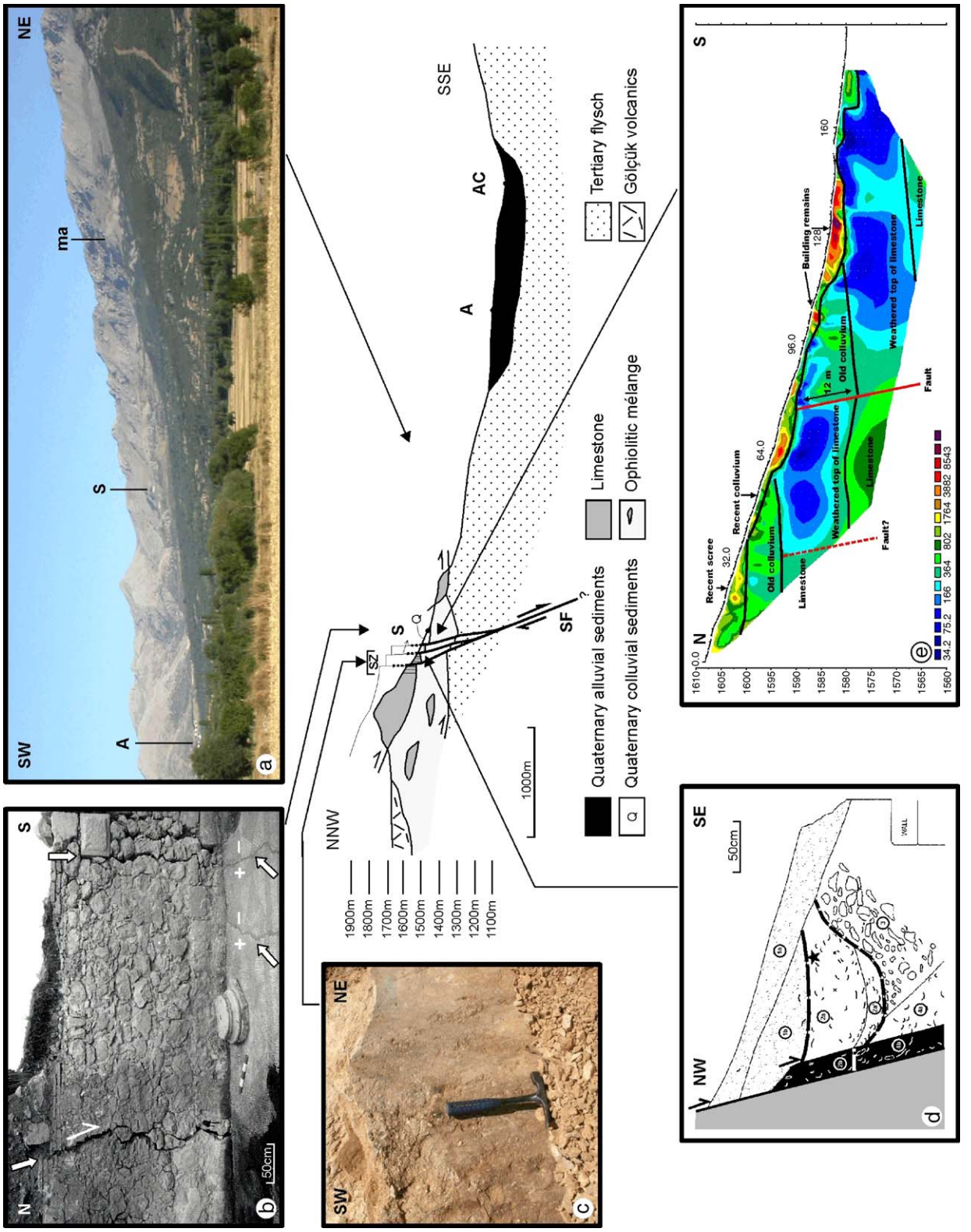
SW
NE
A
S
ma
a
N
S
50cm
b
SW
NE
c
NNW
SSE
1900m
1800m
1700m
1600m
1500m
1400m
1300m
1200m
1100m
1000m
SZ
S
Q
SF
?
A
AC
Quaternary alluvial sediments
Quaternary colluvial sediments
Limestone
Ophiolitic mélange
Tertiary flysch
Gölçük volcanics
S
N
Recent scree
Recent colluvium
Old colluvium
Limestone
Weathered top of limestone
Old colluvium
Limestone
Fault?
Building remains
Fault
Limestone
32.0
64.0
96.0
128
160
12 m
1610
1605
1600
1595
1590
1585
1580
1575
1570
1565
1560
34.2
75.2
166
364
802
1764
3882
8543
e
SE
NW
50cm
WALL
d

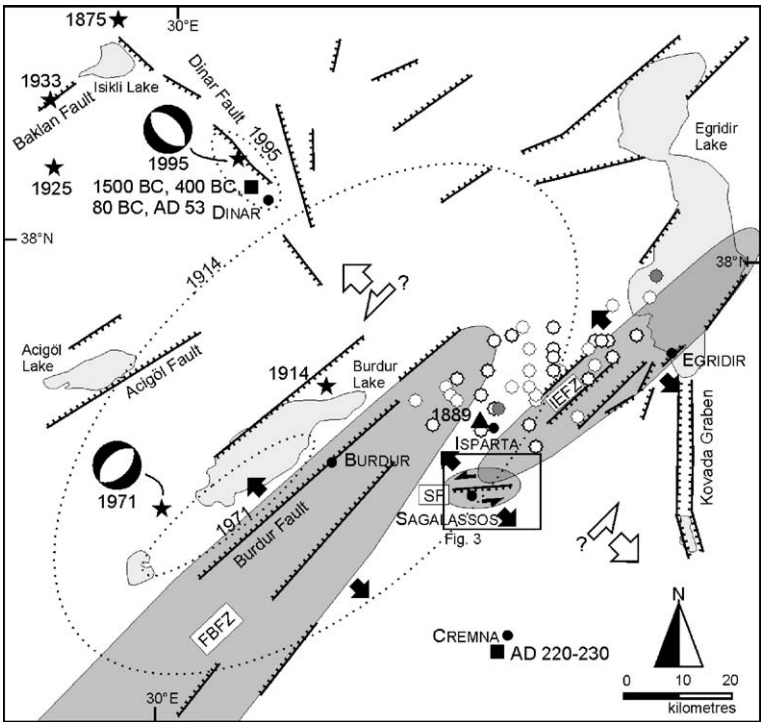

Fig. 7. Conceptual cross-section across the Sagalassos fault based on evidences from the different approaches. The lack of a continuous limestone layer directly in the hanging-wall of the Sagalassos fault is seen as evidence for the presence of large-scale limestone lenses within ophiolitic material. Accordingly, the Sagalassos fault must cross-cut the frontal part of such lenses. The frontal limestones are subsequently heavily degraded and transported down hill. SF: Sagalassos fault; SZ: shatter zone; S: ancient city of Sagalassos; A: village of Ağlasun; AC: Ağlasun Çayı river; ma: massif of the aqueducts. (a) Ağlasun valley, flysch footslopes and limestone mountain range-front. (b) Post-363 AD fractures through the Neon Library. (c) Normal fault plane. (d) Simplified log of the trench showing colluvium (1a–1b), man-made dumps (2a–2a′–3–4a) and post-100 AD sheared fault zone (2b–4b). Black star show location of late Ottoman sherds in unit 2a, small lines represent long axis of pottery fragments and blocks represent major limestone fragments. Upper dashed line indicates the event horizon. Lower dashed line indicates displaced strata along the shear zone (after Similox-Tohon et al., 2005). (e) NS-trending resistivity profile (profile 2 from Similox-Tohon et al., 2004) carried out in front of the Theatre fault segment and directly E of the Roman Theatre (see Fig. 4 for location). Electrode spacing is 2 m, elevations in m a.s.l., vertical exaggeration is 1:1.5, resistivity in ?m and RMS error of the inversion is 3.0.

this geophysical technique does not allow the visualization of individual small-scale colluvial wedges.

7. Palaeoseismological trenching

Once the presence of an active fault is corroborated and the precise location of the fault trace is identified, trenching across the fault enables the study and dating of past earthquakes, especially in areas with archaeological settlements that can provide good dating (e.g. Ellenblum et al., 1998; Galadini and Galli, 1999; Marco et al., 2003). Even though the faults identified in the resistivity profiles at Sagalassos displace recent deposits, trenching at these locations could not be performed due to a large amount of debris covering the archaeological settlement. Therefore a trench has been excavated downslope of limestone front in the eastern part of Necropolis, which may correspond to the degraded main normal fault plane at Sagalassos (Fig. 4). The trench, dug by hand, is ~2 m deep and wide along a N45°E-trending and 65°S-dipping limestone scarp and extends 2.5 m to the southeast. A detailed description of the trench exposure can be found in Similox-Tohon et al. (2005).

The trench, exposing the limestone face and its hanging-wall deposits, reveals a fresh normal fault plane and hence confirms that the limestone cliff at the

Fig. 6. 3D visualization of the 2D resistivity profiles and topography in the eastern sector of ancient Sagalassos site showing identified fault in front of the Theatre fault segment (red lines), displaced top of the weathered bedrock along this fault (black lines), Neon Library (NL) and Roman Theatre (RT). At depth, the profiles indicate the occurrence of a high resistivity layer, interpreted as limestone massif, below the Roman Theatre. Resistivity in ?m, profile length (L) and investigation depth (D) in m.

northwestern extremity of ancient Sagalassos represents a strongly degraded normal fault. Dip–slip frictional-wear striae, tool tracks, spall marks, dilatational fractures, flowstone and an underlying fault breccia have been observed in the excavated part of the limestone cliff. Moreover, in the excavated part of the hanging-wall, evidence of historical reactivation of this fault has been inferred within the anthropogenic deposits (Fig. 7d). The main arguments are the occurrence of a 20-cm thick indurated and compact zone against the limestone face (units 2b and 4b on Fig. 7d), the parallel alignment of ceramics and limestone fragments, dip–slip striae, the displacement of stratigraphic units within an archaeological dump (units 2, 3 and 4 on Fig. 7d), which was deposited at the earliest during the Early Imperial Period (ca. 25 BC–100 AD), and the presence of a post-occupation (post-700 AD?) colluvial wedge (unit 1 on Fig. 7d).

As the shear zone (units 2b and 4b on Fig. 7d) probably formed during one single palaeoseismic event the shear zone and the colluvium wedge (unit 1 on Fig. 7d), associated to a morphogenic earthquake, represents the same event. Two scenarios can be proposed for the timing of this surface-rupturing event based on the occurrence of few intrusive late Ottoman (18th–19th century AD?) sherds (J. Poblome pers. comm. 2003) in the upper part of the dump (unit 2a on Fig. 7d). Firstly, if we assume that the late Ottoman sherds are not likely to have crossed entirely unit 1, it is implied that unit 1a or even whole unit 1 is "post-late Ottoman". Consequently, the possible time window for the palaeoseismic event is constrained between "post-Early Imperial Period" (unit 2a on Fig. 7d) and "post-late Ottoman" (unit 1a on Fig. 7d) or even be "post-late Ottoman" for the case that whole unit 1 would be "post-late Ottoman". However, the hypothesis of a post-late Ottoman event is unlikely because there are no large earthquakes recorded in the catalogues (Ambraseys and Jackson, 1998) and a stong seismic event would have been certainly recorded in the region at that time (post-18th–19th century AD?). Secondly, because pottery fragment intrusion is a common phenomenon, the time window for the palaeoseismic event can be constrained between unit 2a "post-Early Imperial Period" and unit 1 "post-700 AD?/pre-late Ottoman".

8. The Sagalassos fault: a focused picture

The data described above define a coherent picture of the Sagalassos fault (Fig. 7). Each approach contributes in its way to characterize the fault architecture and kinematics. From the integrated approach we show that: (i) the fault is ca. 10 km long and composed of 3 major ENE–WSW-trending right-stepping en-échelon segments; these segments are further composed of minor right-stepping en-échelon fault splays; (ii) the limestone range-front, which has a clear geomorphological expression, represents the (degraded) main Sagalassos fault, while the synthetic faults affecting the Sagalassos site and forming a 150-m wide normal fault zone on the 2D resistivity profiles represent the common hanging-wall migration of fault splays at the surface; (iii) the morphology of the main Sagalassos fault is characteristic of steeply dipping active normal faults cutting bedrock carbonates within the Aegean region; also the vertically displaced bedrock and overlying colluvium observed on the 2D resistivity profiles indicate steeply dipping normal faults; (iv) the stress tensor obtained from the inversion of the striated fault planes indicates a NW–SE extensional regime and is consistent with both the geometry (orientation and segmentation) of the Sagalassos fault and the current stress tensor derived from other Quaternary faults in the region and from focal mechanisms of recent earthquakes; (v) the fractured and faulted inactive scree deposits and part of the mass movements on the south-facing slopes appear to be related to the activity of the Sagalassos fault; (vi) the displaced pre-occupation colluvium, observed on the 2D resistivity profiles is likely related to several pre-occupation surface-rupturing events on the Sagalassos fault; (vii) the displaced archaeological dump, observed in the trench, indicates a historical surface-rupturing event; the possible time window for this palaeoseismic event is constrained between "post-Early Imperial Period" and "post-late Ottoman" or "post-700 AD?/pre-late Ottoman"; (viii) the disrupted aqueduct is possibly related to seismic activity ca. AD 500; (ix) the faulted Neon Library likely indicates a surface-rupturing event after AD 363.

The integrated approach enabled to improve our knowledge of the Sagalassos fault as the causative structure of large pre-historical and historical earthquakes at Sagalassos associated with surface ruptures and extensive damage. The possible time window for the last surface-rupturing event of the main fault (cf. trench) is constrained between "post-Early Imperial Period" and "post-late Ottoman" or "post-700 AD?/pre-late Ottoman". The faults in the Neon Library suggest reactivation of the subsidiary faults observed on the 2D resistivity profiles after the late 4th century AD. We currently assume that this historical surface-rupturing event affected the whole Sagalassos fault zone. Therefore, the time window for the palaeoseismic event can possibly be reduced (late 4th century AD–

post-late Ottoman or post-700 AD?/pre-late Ottoman). Even though the presence of archaeological artifacts provides good dating, the large time window of the palaeoseismic event remains. Hence, an accurate dating of this event cannot be achieved with the present data. Obviously, the historical earthquakes of ca. AD 500 and the middle or second half of the 7th century AD testified in the buildings of Sagalassos could be considered as possible candidates for the palaeoseismic event but this cannot be corroborated and younger unknown events cannot be excluded.

9. Discussion

Even though historical activity on the Sagalassos fault has been proven, the available data set does not give a clear picture of its seismogenic role, i.e. its faulting parameters (Mmax, return period, etc.). A large time window of the palaeoseismic event remains as an accurate dating of this event could not be achieved. Discriminating between the ca. AD 500 and the middle or second half of the 7th century AD earthquakes is not possible. Moreover, it is likely better to think of an earthquake sequence during that period as a cause for the progressive destruction at Sagalassos. The main shock, which should correspond to the surface-rupturing event, may simply have weakened the strength of the buildings to which weaker events may give the final shot (cf. Stiros, 1996). Accordingly, the magnitude of the historical earthquake could not be easily determined. This should be based on enough data concerning the vertical fault displacement of the earthquake. We can only conclude that because the Sagalassos fault is a normal fault in the upper crust of the Aegean region, it is well known that surface faulting occurs for earthquakes of Ms 5.5 and above (cf. Pavlides and Caputo, 2004). This is consistent with the Sagalassos fault length (ca. 10 km) and the intensity ($I \geq$ VIII) based on the earthquake-related damage at Sagalassos. The evaluation of the average slip rate and recurrence of large earthquakes could not be assessed as the age and size of pre-occupation events have not been identified.

The particular orientation of the Sagalassos fault, i.e. ENE–WSW-trending in an area of predominant NE–SW-trending active normal faults, is believed to be related to its geodynamic setting. The Sagalassos fault may be interpreted as part of a fault linkage between the Fethiye–Burdur fault zone (FBFZ) and the Isparta–Eğridir fault zone (IEFZ) (Fig. 2). The IEFZ is seen as the right-lateral overstepping continuation of the FBFZ (Sintubin et al., 2003). The recent and historical seismic activity of these three tectonic structures might indicate their present-day link. (i) This study indicates historical activity on the Sagalassos fault, while (ii) an elongated cluster (17 km wide and 41 km long in a NE–SW-direction) of recent (1900–2000) micro-seismic activity (Md 3.0–4.9) (KOERI, 2002) near the IEFZ might indicate its seismic activity and (iii) recent large earthquakes occurred on the Burdur fault (Fig. 2).

10. Concluding remarks

The identification of a to date unknown seismically active fault, i.e. the Sagalassos fault, is not only a first step in a better understanding of the active tectonics of the area between the FBFZ and the IEFZ, but also a meaningful contribution to a more reliable assessment of the seismic hazard in the Burdur–Isparta area. As the FBFZ and the IEFZ are characterized by seismic activity during the past century, the hypothesis of future reactivations of the Sagalassos fault with similar seismic events as evidenced in this study and due to the evolving fault linkage process cannot be neglected.

The present study illustrates how the use of a multidisciplinary approach integrating archaeoseismological evidences enables to better constrain the architecture of a fault zone and to demonstrate its activity.

Acknowledgments

We would like to thank R. Caputo and an anonymous referee for the constructive review of the manuscript. This research is supported by a Concerted Action of the Flemisch Government (GOA 02/2) and the Interuniversity Attraction Poles Programme — Belgian Science Policy (IUAP P5/09). M. Sintubin is a Research Associate of the Onderzoeksfonds at the K.U.Leuven. S. Vandycke is a Research Associate of the National Research Foundation of Belgium (FNRS). H. Vanhaverbeke is a postdoctoral Fellow with the Fund for Scientific Research — Flanders (Belgium). M. Waelkens is L. Baert-Hofman Professor in Eastern Mediterranean Archaeology.

References

Akyüz, H.S., Altunel, E., 2001. Geological and archaeological evidence for post-Roman earthquake surface faulting at Cibyra, SW Turkey. Geodinamica Acta 14, 95–101.

Altunel, E., 1998. Evidence for damaging historical earthquakes at Priene, Western Turkey. Turkish Journal of Earth Sciences 7, 25–35.

Altunel, E., Barka, A.A., Akyüz, H.S., 1999. Palaeoseismicity of the Dinar fault, SW Turkey. Terra Nova 11, 297–302.

Altunel, E., Stewart, I.S., Barka, A.A., Piccardi, L., 2003. Earthquake faulting at ancient Cnidus, SW Turkey. Turkish Journal of Earth Sciences 12 (1), 137–151.

Ambraseys, N.N., 2001. Reassessment of earthquakes, 1900–1999, in the Eastern Mediterranean and the Middle East. Geophysical Journal International 145, 471–485.

Ambraseys, N.N., Jackson, J.A., 1998. Faulting associated with historical and recent earthquakes in the eastern Mediterranean region. Geophysical Journal International 133, 390–406.

Angelier, J., 1984. Tectonic analysis of fault slip data sets. Journal of Geophysical Research 89, 5835–5848.

Barka, A.A., Reilinger, R., 1997. Active tectonics of the eastern Mediterranean region: deduced from GPS, neotectonics and seismicity data. Annali di Geofisica 40, 587–610.

Barka, A.A., Reilinger, R., Saroglu, F., Sengör, A.M.C., 1995. The Isparta Angle: its importance in the neotectonics of the Eastern Mediterranean Region. In: Piskin, D., Ergun, M., Savasçin, M.Y., Tarcan, G. (Eds.), International Earth Sciences Colloquium on the Aegean Region. Dokus Eylul University, Izmir, Turkey, pp. 3–18.

Blumenthal, M.M., 1963. Le système structural du Taurus sud Anatolien. Mémoires de la Société Géologique de France 1 (2), 611–662.

Bozkurt, E., 2001. Neotectonics of Turkey — a synthesis. Geodinamica Acta 14, 3–30.

Caputo, R., 1993. Morphogenic earthquakes: a proposal. Bull. INQUA-NC 16, 24.

Caputo, R., 1996. The active Nea Anchialos Fault System (Central Greece): comparison of geological, morphotectonic, archaeological and seismological data. Annali di Geofisica 39 (3), 1–17.

Collettini, C., Barchi, M.R., Chiaraluce, L., Mirabella, F., Pucci, S., 2003. The Gubbio fault: can different methods give pictures of the same object? Journal of Geodynamics 36, 51–66.

Collins, A.S., Robertson, A.H.F., 1997. Lycian melange, southwestern Turkey: an emplaced Late Cretaceous accretionary complex. Geology 25 (3), 255–258.

Degryse, P., Muchez, P., Sintubin, M., Clijsters, A., Viaene, W., Dederen, M., Schrooten, P., Waelkens, M., in press. Geological mapping of the area around Sagalassos (SW Turkey). In: Waelkens, M., Poblome, J. (Eds.), Sagalassos VI. Acta Archaeologica Lovaniensia Monographiae. University Press, Leuven.

Ellenblum, R., Marco, S., Agnon, A., Rockwell, T., Boas, A., 1998. Crusader castle torn apart by earthquake at dawn, 20 May 1202. Geology 26 (4), 303–306.

Emre, Ö., Duman, T.Y., Dogan, A., Özalp, S., Tokay, F., Kusçu, I., 2003. Surface faulting associated with the Sultandagi earthquake (Mw 6.5) of 3 February 2002, Southwestern Turkey. Seismological Research Letters 74 (4), 382–392.

Eyidoğan, H., Barka, A.A., 1996. The 1 October 1995 Dinar earthquake, SW Turkey. Terra Nova 8, 479–485.

Galadini, F., Galli, P., 1999. Palaeoseismology related to the displaced Roman archaeological remains at Egna (Adige Valley, northern Italy). Tectonophysics 308, 171–191.

Galli, P., Galadini, F., 2001. Surface faulting of archaeological relics. A review of case histories from the Dead Sea to the Alps. Tectonophysics 335, 291–312.

Glover, C., Robertson, A.H.F., 1998. Neotectonic intersection of the Aegean and Cyprus tectonic arcs: extensional and strike–slip faulting in the Isparta Angle, SW Turkey. Tectonophysics 298, 103–132.

Goldsworthy, M., Jackson, J., 2000. Active normal fault evolution in Greece revealed by geomorphology and drainage patterns. Journal of the Geological Society (London) 157, 967–981.

GSHAP, 2004. Global Seismic Hazard Assessment Program. http://www.seismo.ethz.ch/GSHAP/ (accessed December 2004).

Hancock, P.L., Altunel, E., 1997. Faulted Archaeological Relics at Hierapolis (Pamukkale), Turkey. In: Hancock, P.L., Michetti, A.M. (Eds.), Paleoseismology: Understanding Past Earthquakes Using Quaternary Geology. Journal of Geodynamics, pp. 21–36.

Ignoul, S., Van Gemert, D., 1999. Sagalassos Excavation Project: Roman Baths, Technology Restoration Innovation Consult, 3294 Diest.

Kahle, H.-G., Cocard, M., Peter, Y., Geiger, A., Reilinger, R., McClusky, S.C., King, A., Barka, A.A., Veis, G., 1999. The GPS strain rate field in the Aegean Sea and Western Anatolia. Geophysical Research Letters 26, 2513–2516.

Karcz, I., Kafri, U., 1978. Evaluation of supposed archaeoseismic damage in Israel. Journal of Archaeological Science 5, 237–253.

KOERI, 2002. Kandili Observatory and Earthquake Research Institute earthquake catalogue. http://www.koeri.boun.edu.tr/jeofizik/mapeng.htm (accessed September 2002).

Koral, H., 2000. Surface rupture and rupture mechanism of the October 1, 1995 (M_w=6.2) Dinar earthquake, SW Turkey. Tectonophysics 327, 15–24.

Korjenkov, A.M., Mazor, E., 1999a. Earthquake characteristics reconstructed from archeological damage patterns: Shivta, the Negev Desert, Israel. Israel Journal of Earth-Sciences 48, 265–282.

Korjenkov, A.M., Mazor, E., 1999b. Seismogenic origin of the ancient Avdat ruins, Negev Desert, Israel. Natural Hazards 18, 193–226.

Librecht, I., Paulissen, E., Verstraeten, G., Waelkens, M., 2000. Implications of Environmental Changes on Slope Evolution Near Sagalassos. In: Waelkens, M., Loots, L. (Eds.), Sagalassos V. Report on the Survey and Excavation Campaigns of 1996 and 1997. Acta Archaeologica Lovaniensia Monographiae, vol. 11. University Press, Leuven, pp. 799–817.

Marco, S., Hartal, M., Hazan, N., Lev, L., Stein, M., 2003. Archaeology, history, and geology of the A.D. 749 earthquake, Dead Sea transform. Geology 31 (8), 665–668.

Michetti, A.M., Hancock, P.L., 1997. Paleoseismology: understanding past earthquakes using quaternary geology. In: Hancock, P.L., Michetti, A.M. (Eds.), Paleoseismology: Understanding Past Earthquakes Using Quaternary Geology. Journal of Geodynamics, vol. 24(1–4), pp. 3–10.

Michetti, A.M., Audemard, M., F.A., Marco, S., 2005. Future trends in paleoseismology: integrated study of the seismic landscape as a vital tool in seismic hazard analyses. Tectonophysics 408 (1–4), 3–21.

Paulissen, E., Poesen, J., Govers, G., De Ploey, J., 1993. The Physical Environment at Sagalassos (Western Taurus, Turkey). A Reconnaissance Survey. In: Waelkens, M., Poblome, J. (Eds.), Sagalassos: II. Report on the Third Excavation Campaign of 1992. Acta Archaeologica Lovaniensia Monographiae, vol. 6. University Press, Leuven, pp. 229–249.

Pavlides, S., Caputo, R., 1994. The North Aegean region: a tectonic paradox? Terra Nova 6 (1), 37–44.

Pavlides, S., Caputo, R., 2004. Magnitude versus faults' surface parameters: quantitative relationships from the Aegean Region. Tectonophysics 380, 159–188.

Price, S.P., Scott, B., 1991. Pliocene Burdur basin, SW Turkey: tectonics, seismicity and sedimentation. Journal of the Geological Society (London) 148, 345–354.

Price, S.P., Scott, B., 1994. Fault-block rotations at the edge of a zone of continental extension: southwest Turkey. Journal of Structural Geology 16 (3), 381–392.

Rapp, G., 1986. Assessing archaeological evidence for seismic catastrophies. Geoarchaeology 1 (4), 365–379.

Robertson, A.H.F., 1993. Mesozoic-Tertiary sedimentary and tectonic evolution of Neotethyan carbonate platforms, margins and small ocean basins in the Antalya Complex, southwest Turkey. Special Publication of the International Association of Sedimentologists 20, 415–465.

Şenel, M., 1997. Geological map of the Isparta — J11 Quadrangle. General Directorate of Mineral Research and Exploration, Ankara.

Similox-Tohon, D., Vanneste, K., Sintubin, M., Muchez, P., Waelkens, M., 2004. Two-dimensional resistivity imaging: a tool in archaeo-seismology. An example from ancient Sagalassos (SW Turkey). Archaeological Prospection 11 (1), 1–18.

Similox-Tohon, D., Sintubin, M., Muchez, P., Vanhaverbeke, H., Verhaert, G., Waelkens, M., 2005. Identification of a historical morphogenic earthquake through trenching at ancient Sagalassos (SW Turkey). Journal of Geodynamics 40, 279–293.

Sintubin, M., Muchez, P., Similox-Tohon, D., Verhaert, G., Paulissen, E., Waelkens, M., 2003. Seismic catastrophes at the ancient city of Sagalassos (SW Turkey) and their implications for the seismotectonics in the Burdur–Isparta area. Geological Journal 38, 359–374.

Six, S., 2004. Holocene geomorphological evolution of the territory of Sagalassos. Unpublished doct. thesis, Katholieke Universiteit Leuven, Leuven. 242 pp.

Steegen, A., Cauwenberghs, K., Govers, G., Waelkens, M., Owens, E. J., Desmet, P., 2000. The Water Supply to Sagalassos. In: Waelkens, M., Loots, L. (Eds.), Sagalassos V. Report on the Survey and Excavation Campaigns of 1996 and 1997. Acta Archaeologica Lovaniensia Monographiae, vol. 11. University Press, Leuven, pp. 635–649.

Stewart, I.S., 1996. A rough guide to limestone fault scarps. Journal of Structural Geology 18 (10), 1259–1264.

Stewart, I.S., Hancock, P.L., 1988. Normal fault zone evolution and fault scarp degradation in the Aegean region. Basin Research 1, 139–153.

Stewart, I.S., Hancock, P.L., 1990. Brecciation and Fracturing Within Neotectonic Normal Fault Zones in the Aegean Region. In: Knipe, R.J., Rutter, E.H. (Eds.), Deformation Mechanisms, Rheology and Tectonics. Geological Society, London, Special Publication, pp. 105–112.

Stiros, S.C, 1996. Identification of earthquakes from archaeological data: methodology, criteria and limitations. In: Stiros, S.C., Jones, R.E. (Eds.), Archaeoseismology. Fitch Laboratory Occasional Paper, vol. 7. Institute of Geology and Mineral Exploration and The British School at Athens, Athens, pp. 129–152.

Taymaz, T., Price, S., 1992. The 1971 May 12 Burdur earthquake sequence, SW Turkey: a synthesis of seismological observations. Geophysical Journal International 108, 589–603.

Temiz, H., Poisson, A., Andrieux, J., 2001. The Plio-Quaternary Extensional System of the Western Side of the Isparta Angle in SW Turkey. 4th International Symposium on Eastern Mediterranean Geology, Isparta, Turkey, pp. 125–129.

ten Veen, J.H., 2004. Extension on Hellenic forearc shear zones in SW Turkey: the Pliocene-Quaternary deformation of the Esen Cay Basin. Journal of Geodynamics 37, 181–204.

ten Veen, J.H., Kleinspehn, K.L., 2002. Geodynamics along an increasingly curved convergent plate margin: Late Miocene–Pleistocene Rhodes, Greece. Tectonics 21 (3), 8–1–8–21.

ten Veen, J.H., Kleinspehn, K.L., 2003. Incipient continental collision and plate-boundary curvature: Late Pliocene–Holocene transtensional Hellenic forearc, Crete, Greece. Journal of the Geological Society (London) 160, 161–181.

Van de Velde, P., 1998. Verwering van kalkstenen in het gebied van Sagalassos (Turkije). M. Sc. Thesis, Katholieke Universiteit Leuven, Leuven. 100 pp.

Verhaert, G., Muchez, P., Sintubin, M., Similox-Tohon, D., Vandycke, S., Kepens, E., Hodge, E.J., Richards, D.A., 2004. Origin of palaeofluids in a normal fault setting in the Aegean region. Geofluids 4, 300–314.

Verstraeten, G., Paulissen, E., Librecht, I., Waelkens, M., 2000. Limestone Platforms Around Sagalassos Resulting from Giant Mass Movements. In: Waelkens, M., Loots, L. (Eds.), Sagalassos V. Report on the Survey and Excavation Campaigns of 1996 and 1997. Acta Archaeologica Lovaniensia Monographiae, vol. 11. University Press, Leuven, pp. 783–798.

Waelkens, M., Sintubin, M., Muchez, P., Paulissen, E., 2000. Archeological, Geomorphological and Geological Evidence for a Major Earthquake at Sagalassos (SW Turkey) Around the Middle of the Seventh Century AD. In: McGuire, W.J., Griffiths, D.R., Hancock, P.L., Stewart, I.S. (Eds.), The Archaeology of Geological Catastrophes. Geological Society, London, Special Publication, pp. 373–383.